JOURNAL OF THEORETICAL AND APPLIED MECHANICS
50, 3, pp. 831-839, Warsaw 2012
50th Anniversary of JTAM

TRANSIENT THERMOELASTIC ANALYSIS FOR A FUNCTIONALLY GRADED CIRCULAR DISK WITH PIECEWISE POWER LAW

Naotake Noda

Professor Emeritus, Department of Mechanical Engineering, Shizuoka University, Japan; e-mail: naotakenoda@yahoo.co.jp

Yoshihiro Ootao

Department of Mechanical Engineering, Graduate School of Engineering, Osaka Prefecture University, Japan; e-mail: ootao@me.osakafu-u.ac.jp

Yoshinobu Tanigawa

Professor Emeritus, Department of Mechanical Engineering, Graduate School of Engineering, Osaka Prefecture University, Japan; e-mail: tanigawayoshinobu20070424@zeus.eonet.ne.jp

The theoretical treatment of a transient thermoelastic problem involving a functionally graded solid circular disk with piecewise power law due to uniform heat supply from an outer surface is studied. The solid circular disk is also cooled from the upper and lower flat surfaces. The functionally graded circular disk consists of many thin circular layers in order to guarantee the voluntariness of material position dependency. The thermal conductivity, Young's modulus and the coefficient of linear thermal expansion of each layer, except the first inner layer, are expressed as power functions of the radial coordinate, and their values continue on the interfaces. We obtain the exact solution for the one-dimensional temperature change in a transient state, and in-plane thermoelastic response under the state of plane stress. Some numerical results for the temperature change, displacement and stress distributions are shown in figures.

Key words: functionally graded material, solid circular disk, piecewise power law

1. Introduction

Functionally graded materials (FGMs) are those in which two or more different material ingredients change continuously and gradually along the certain direction. When FGMs are used under high temperature conditions or are subjected to several thermal loading, it is necessary to analyze the thermal stress problems for FGMs. Because the governing equations for the temperature field and the associate thermoelastic field of FGMs become of a nonlinear form in generally, the analytical treatment is difficult. Noda and Tsuji (1991) analyzed the steady thermoelastic problem of an FGM plate. Peng and Li (2010) analyzed the steady thermal stress problem in rotating FGM hollow circular disks.

On the other hand, it is well-known that thermal stress distributions in a transient state can show large values compared with the one in a steady state. Therefore, the analysis of the transient thermoelastic problem for FGMs becomes important. Obata and Noda (1995) analyzed the transient thermal stresses in a hollow sphere of FGM by the perturbation method. The other exact analytical treatments are assumed that the material properties are given by specific functions containing the variable of the thickness coordinate. Sugano (1987) analyzed exactly one-dimensional transient thermal stresses of an FGM plate where the thermal conductivity and Young's modulus vary exponentially, whereas Poisson's ratio and the coefficient of linear thermal expansion vary arbitrarily in the thickness direction. Vel and Batra (2003) analyzed the three-dimensional transient thermal stresses of an FGM rectangular plate, where the material

properties are expressed as Taylor's series in the thickness direction. Ootao and Tanigawa (2005) discussed the three-dimensional transient thermal stress problems of an FGM rectangular plate, where the thermal conductivity, the coefficient of linear thermal expansion and Young's modulus vary exponentially in the thickness direction. Ohmichi *et al.* (2010) analyzed the transient thermal stress problem of the strip with boundaries oblique to the functionally graded direction. Zhao *et al.* (2006) treated the one-dimensional transient thermo-mechanical behavior of FGM solid cylinder, whose thermoelastic material properties vary exponentially through the thickness. Ootao and Tanigawa (2006) analyzed the one-dimensional solution for transient thermal stresses of an FGM hollow cylinder whose material properties vary with the power product form of the radial coordinate variable. Shao *et al.* (2007) discussed the one-dimensional transient thermo-mechanical behavior of FGM hollow cylinders, whose thermoelastic material properties are expressed as Taylor's series.

However, these studies discussed the thermoelastic problems of one-layered FGM models, which have big limitation of nonhomogeneity. Tanigawa *et al.* (1989) proposed the theory of laminated composites whose material properties have constants in each layer. Ootao and Tanigawa (1994, 1999), Ootao *et al.* (1995), and Sugano *et al.* (2001) analyzed the transient thermal stress problems of several analytical models using the theory of laminated composites. But the theory of laminated composites has a weak point such that the material properties are discontinuous on each interface. Guo and Noda (2007) proposed a piecewise-exponential model for the crack problems in FGMs with arbitrary material properties which are continuous on each interface in order to improve the ordinary theory of laminated composites. Ootao (2010) analyzed the transient thermoelastic problem in the FGM hollow cylinder by a piecewise-power model when the material properties can be expressed by piecewise power law.

From the viewpoint of past studies, we analyze the transient thermoelastic analysis for an FGM solid circular disk whose material properties are expressed by piecewise power law to guarantee arbitrary nonhomogeneity of material properties. The FGM disk is suddenly heated from the outer surface by surrounding media, and also is cooled from the upper and lower surfaces.

2. Analysis

The functionally graded solid circular disk consists of many layers whose material properties are expressed by piecewise power law of position. The thermal conductivity, Young's modulus and the coefficient of linear thermal expansion of each layer, except the first inner layer, are expressed as power functions of the radial coordinate, and their values continue on each interface. The outer radius of the solid circular disk is designated by r_b. Moreover, r_i is the outer radius of the ith layer. The thickness of the solid circular disk is represented by B.

2.1. Heat conduction problem

The FGM circular disk is assumed to be initially at zero temperature and is suddenly heated from the outer surface by surrounding media of constant temperature T_b with relative heat transfer coefficient h_b. The FGM circular disk is also cooled from the upper and lower surfaces of the ith layer by the surrounding media of zero temperature with the heat transfer coefficient γ_{is}. The one-dimensional transient heat conduction equation for the ith layer is taken in the following form

$$c_i\rho_i\frac{\partial T_i}{\partial t} = \frac{1}{r}\frac{\partial}{\partial r}\Big[\lambda_i(r)r\frac{\partial T_i}{\partial r}\Big] - \frac{2\gamma_{si}}{B}T_i \qquad i = 1, 2, \ldots, N \tag{2.1}$$

The thermal conductivity λ_i and the heat capacity per unit volume $c_i\rho_i$ in each layer are assumed to take the following forms

$$\lambda_i(r) = \begin{cases} \lambda_i(\,\text{const}\,) & \text{for} \quad i = 1 \qquad c_i\rho_i = \text{const} \\ \lambda_i^0\Big(\dfrac{r}{r_{i-1}}\Big)^{m_i} & \text{for} \quad i = 2,\ldots,N \qquad c_i\rho_i = \text{const} \end{cases} \tag{2.2}$$

where

$$m_i = \frac{\ln(\overline{\lambda}_{i+1}{}^0/\overline{\lambda}_i{}^0)}{\ln(\overline{r}_i/\overline{r}_{i-1})} \qquad \lambda_1 = \lambda_2{}^0 \qquad c_i\rho_i \neq c_{i+1}\rho_{i+1} \tag{2.3}$$

Substituting Eqs. (2.2) into Eq. (2.1), the transient heat conduction equations in dimensionless form for each layer are

$$\frac{\partial\overline{T}_i}{\partial\tau} = \begin{cases} \overline{\kappa}_i\Big(\dfrac{\partial^2\overline{T}_i}{\partial\overline{r}^2} + \dfrac{1}{\overline{r}}\dfrac{\partial\overline{T}_i}{\partial\overline{r}}\Big) - \dfrac{2H_{si}}{\overline{c}_i\overline{\rho}_i\overline{B}}\overline{T}_i & \text{for} \quad i = 1 \\ \dfrac{\overline{\lambda}_i^0}{\overline{c}_i\overline{\rho}_i\overline{r}_{i-1}^{m_i}}\Big(\overline{r}^{m_i}\dfrac{\partial^2\overline{T}_i}{\partial\overline{r}^2} + (m_i+1)\overline{r}^{m_i-1}\dfrac{\partial\overline{T}_i}{\partial\overline{r}}\Big) - \dfrac{2H_{si}}{\overline{c}_i\overline{\rho}_i\overline{B}}\overline{T}_i & \text{for} \quad i = 2,\ldots,N \end{cases} \tag{2.4}$$

The initial and thermal boundary conditions in dimensionless form are

$$\tau = 0 \qquad \overline{T}_i = 0 \qquad i = 1,2,\ldots,N \tag{2.5}$$

and

$$\begin{aligned} &\overline{r} = \overline{r}_i \qquad \overline{T}_i = \overline{T}_{i+1} && i = 1,2,\ldots,N-1 \\ &\overline{r} = \overline{r}_i \qquad \overline{\lambda}_i\frac{\partial\overline{T}_i}{\partial\overline{r}} = \overline{\lambda}_{i+1}\frac{\partial\overline{T}_{i+1}}{\partial\overline{r}} && i = 1,2,\ldots,N-1 \\ &\overline{r} = 1 \qquad \frac{\partial\overline{T}_N}{\partial\overline{r}} + H_b\overline{T}_N = H_b\overline{T}_b \end{aligned} \tag{2.6}$$

In Eqs. (2.4)-(2.6), we have introduced the following dimensionless values

$$\begin{aligned} &(\overline{T}_i,\overline{T}_a,\overline{T}_b) = \frac{(T_i,T_a,T_b)}{T_0} && (\overline{r},\overline{r}_i,\overline{B}) = \frac{(r,r_i,B)}{r_b} && \tau = \frac{\lambda_0 t}{c_0\rho_0 r_b^2} \\ &\overline{c}_i\overline{\rho}_i = \frac{c_i\rho_i}{c_0\rho_0} && (\overline{\lambda}_i,\overline{\lambda}_i^0) = \frac{(\lambda_i,\lambda_i^0)}{\lambda_0} && \overline{\kappa}_i = \frac{\overline{\lambda}_i}{\overline{c}_i\overline{\rho}_i} \\ &H_b = h_b r_b && H_{si} = \frac{\gamma_{si} r_b}{\lambda_0} \end{aligned} \tag{2.7}$$

where T_i is the temperature change; t is time; and T_0, λ_0 and $c_0\rho_0$ are typical values of temperature, thermal conductivity and heat capacity per unit volume, respectively. Introducing the Laplace transformation with respect to the variable τ, solutions to Eqs. (2.4) can be obtained so as to satisfy conditions (2.5) and (2.6). These solutions are shown as follows:
— for $i = 1$

$$\begin{aligned} \overline{T}_i = {} & \frac{1}{F}\overline{A}_i' I_0(\omega_i'\overline{r}) \\ & + \sum_{j=1}^{\infty}\Big\{\frac{2\overline{\lambda}_2^0\overline{B}\mu_{2j}(2-m_2)^2}{[\mu_{2j}^2\overline{\lambda}_2^0(2-m_2)^2\overline{B} + 8H_{s2}\overline{r}_1^{m_2}]\Delta'(\mu_{2j})}\exp\Big[-\Big(\frac{\overline{\lambda}_2^0(2-m_2)^2\mu_{2j}^2}{4\overline{c}_2\overline{\rho}_2\overline{r}_1^{m_2}} + \frac{2H_{s2}}{\overline{c}_2\overline{\rho}_2\overline{B}}\Big)\tau\Big] \\ & \cdot \overline{A}_i J_0\Big(\sqrt{M_{1i}'\mu_{2j}^2 + M_{2i}'}\,\overline{r}\Big)\Big\} \end{aligned} \tag{2.8}$$

— for $i = 2, \ldots, N$

$$\begin{aligned}\overline{T}_i = {} & \frac{1}{F}\overline{r}^{-\frac{m_i}{2}}\Big[\overline{A}'_i I_{\gamma_i}(\omega_i \overline{r}^{1-\frac{m_i}{2}}) + \overline{B}'_i K_{\gamma_i}(\omega_i \overline{r}^{1-\frac{m_i}{2}})\Big] \\ & + \sum_{j=1}^{\infty}\Big\{ \frac{2\overline{\lambda}_2^0 \overline{B}\mu_{2j}(2-m_2)^2 \overline{r}^{-\frac{m_i}{2}}}{[\mu_{2j}^2 \overline{\lambda}_2^0 (2-m_2)^2 \overline{B} + 8H_{s2}\overline{r}_1^{m_2}]\Delta'(\mu_{2j})} \exp\Big[-\Big(\frac{\overline{\lambda}_2^0(2-m_2)^2\mu_{2j}^2}{4\overline{c}_2\overline{\rho}_2\overline{r}_1^{m_2}} + \frac{2H_{s2}}{\overline{c}_2\overline{\rho}_2\overline{B}}\Big)\tau\Big] \\ & \cdot \Big[\overline{A}_i J_{\gamma_i}\Big(\sqrt{M_{1i}\mu_{2j}^2 + M_{2i}}\,\overline{r}^{1-\frac{m_i}{2}}\Big) + \overline{B}_i Y_{\gamma_i}\Big(\sqrt{M_{1i}\mu_{2j}^2 + M_{2i}}\,\overline{r}^{1-\frac{m_i}{2}}\Big)\Big]\Big\}\end{aligned} \tag{2.9}$$

where $I_\xi(\cdot)$ and $K_\xi(\cdot)$ are the modified Bessel functions of the first and second kind of the order ξ, respectively. $J_\xi(\cdot)$ and $Y_\xi(\cdot)$ are the Bessel functions of the first and second kind of the order ξ, respectively. And Δ and F are the determinants of $(2N-1)\times(2N-1)$ matrix $[a_{kl}]$ and $[e_{kl}]$, respectively. The coefficients $\overline{A}_1$, $\overline{A}_i$ $(i = 2, \ldots, N)$ and $\overline{B}_i$ $(i = 2, \ldots, N)$ are defined as the determinant of the matrix similar to the coefficient matrix $[a_{kl}]$, in which the first column, $(2i-2)$th column or $(2i-1)$th column is replaced by the constant vector $\{c_k\}$, respectively. Similarly, the coefficients $\overline{A}'_1$, $\overline{A}'_i$ $(i = 2, \ldots, N)$ and $\overline{B}'_i$ $(i = 2, \ldots, N)$ are defined as the determinant of the matrix similar to the coefficient matrix $[e_{kl}]$, in which the first column, $(2i-2)$th column or $(2i-1)$th column is replaced by the constant vector $\{c_k\}$, respectively. The elements of the coefficient matrices $[a_{kl}]$, $[e_{kl}]$ and the constant vector $\{c_k\}$ are given by Eqs. (2.6). In Eqs. (2.8) and (2.9), M'_{1i}, M'_{2i}, M_{1i}, M_{2i}, $\Delta'(\mu_{2j})$, ω'_i, ω_i and γ_i are

$$\begin{aligned} M'_{1i} &= \frac{\overline{\lambda}_2^0(2-m_2)^2}{4\overline{c}_2\overline{\rho}_2\overline{r}_1^{m_2}\overline{\kappa}_i} & M'_{2i} &= \frac{2}{\overline{B}\overline{\kappa}_i}\Big(\frac{H_{s2}}{\overline{c}_2\overline{\rho}_2} - \frac{H_{si}}{\overline{c}_i\overline{\rho}_i}\Big) \\ M_{1i} &= \frac{\overline{\lambda}_2^0(2-m_2)^2\overline{c}_i\overline{\rho}_i\overline{r}_{i-1}^{m_i}}{\overline{\lambda}_i^0(2-m_i)^2\overline{c}_2\overline{\rho}_2\overline{r}_1^{m_2}} & M_{2i} &= \frac{8\overline{c}_i\overline{\rho}_i\overline{r}_{i-1}^{m_i}}{\overline{\lambda}_i^0(2-m_i)^2\overline{B}}\Big(\frac{H_{s2}}{\overline{c}_2\overline{\rho}_2} - \frac{H_{si}}{\overline{c}_i\overline{\rho}_i}\Big) \\ \Delta'(\mu_{2j}) &= \frac{d\Delta}{d\mu_2}\Big|_{\mu_2=\mu_{2j}} & \omega'_i &= \sqrt{\frac{2H_{si}}{\overline{\lambda}_i\overline{B}}} \\ \omega_i &= \sqrt{\frac{8H_{si}\overline{r}_{i-1}^{m_i}}{\overline{\lambda}_i^0\overline{B}(2-m_i)^2}} & \gamma_i &= \Big|\frac{m_i}{2-m_i}\Big| \end{aligned} \tag{2.10}$$

and μ_{2j} represent the jth positive roots of the following transcendental equation

$$\Delta(\mu_2) = 0 \tag{2.11}$$

2.2. Thermoelastic problem

The transient thermoelasticity of the FGM disk is analyzed under the plane stress problem. The displacement-strain relations are expressed in the dimensionless form as follows

$$\overline{\varepsilon}_{rri} = \overline{u}_{ri,\overline{r}} \qquad \overline{\varepsilon}_{\theta\theta i} = \frac{\overline{u}_{ri}}{\overline{r}} \tag{2.12}$$

where the comma denotes partial differentiation with respect to the variable that follows. The constitutive relations are in the dimensionless form as follows

$$\begin{Bmatrix}\overline{\sigma}_{rri}\\ \overline{\sigma}_{\theta\theta i}\end{Bmatrix} = \frac{\overline{E}_i}{(1+\nu_i)(1-\nu_i)}\begin{bmatrix}1 & \nu_i\\ \nu_i & 1\end{bmatrix}\begin{Bmatrix}\overline{\varepsilon}_{rri}\\ \overline{\varepsilon}_{\theta\theta\, i}\end{Bmatrix} - \frac{\overline{\alpha_i}\overline{E}_i\overline{T}_i}{1-\nu_i} \tag{2.13}$$

The equilibrium equation is expressed in the dimensionless form as follows

$$\overline{\sigma}_{rri,\overline{r}} + \frac{1}{\overline{r}}(\overline{\sigma}_{rri} - \overline{\sigma}_{\theta\theta i}) = 0 \tag{2.14}$$

Young's modulus E_i, the coefficient of linear thermal expansion α_i and Poisson's ratio ν_i are assumed to take the following forms: — for $i = 1$

$$\overline{E}_i(\overline{r}) = \overline{E}_i(\text{ const }) \qquad \overline{\alpha}_i(\overline{r}) = \overline{\alpha}_i(\text{ const }) \qquad \nu_i = \text{ const} \tag{2.15}$$

— for $i = 2, \ldots, N$

$$\overline{E}_i(\overline{r}) = \overline{E}_i^0\Big(\frac{\overline{r}}{\overline{r}_{i-1}}\Big)^{l_i} \qquad \overline{\alpha}_i(\overline{r}) = \overline{\alpha}_i^0\Big(\frac{\overline{r}}{\overline{r}_{i-1}}\Big)^{b_i} \qquad \nu_i = \text{ const} \tag{2.16}$$

where

$$\begin{aligned} &l_i = \frac{\ln(\overline{E}_{i+1}^0/\overline{E}_i^0)}{\ln(\overline{r}_i/\overline{r}_{i-1})} \qquad b_i = \frac{\ln(\overline{\alpha}_{i+1}^0/\overline{\alpha}_i^0)}{\ln(\overline{r}_i/\overline{r}_{i-1})} \\ &\overline{E}_1 = \overline{E}_2^0 \qquad \overline{\alpha}_1 = \overline{\alpha}_2^0 \qquad \nu_i \neq \nu_{i+1} \end{aligned} \tag{2.17}$$

In Eqs. (2.12)-(2.17), the following dimensionless values are introduced

$$\begin{aligned} &\overline{\sigma}_{kli} = \frac{\sigma_{kli}}{\alpha_0 E_0 T_0} \qquad \overline{\varepsilon}_{kli} = \frac{\varepsilon_{kli}}{\alpha_0 T_0} \qquad (\overline{\alpha}_i, \overline{\alpha}_i^0) = \frac{(\alpha_i, \alpha_i^0)}{\alpha_0} \\ &(\overline{E}_i, \overline{E}_i^0) = \frac{(E_i, E_i^0)}{E_0} \qquad \overline{u}_{ri} = \frac{u_{ri}}{\alpha_0 T_0 r_b} \end{aligned} \tag{2.18}$$

where σ_{kli} are the stress components, ε_{kli} are the strain components, u_{ri} is the displacement in the radial direction, and α_0 and E_0 are typical values of the coefficient of linear thermal expansion and Young's modulus, respectively. Substitution of Eqs. (2.12), (2.13), (2.15) and (2.16) into Eq. (2.14) gives the displacement equation of equilibrium for $i = 2, \ldots, N$

$$\overline{u}_{ri,\overline{r}\overline{r}} + \frac{l_i + 1}{\overline{r}}\overline{u}_{ri,\overline{r}} + (\nu_i l_i - 1)\overline{u}_{ri}\overline{r}^{-2} = \frac{(1+\nu_i)\overline{\alpha}_i^0}{\overline{r}_{i-1}^{b_i}}[(l_i + b_i)\overline{r}^{b_i - 1}\overline{T}_i + \overline{r}^{b_i}\overline{T}_{i,\overline{r}}] \tag{2.19}$$

If the outer surface is traction free, and the interfaces of each layer are perfectly bonded, then the boundary conditions of the outer surface and the conditions of continuity on the interfaces can be represented as follows

$$\begin{aligned} &\overline{r} = 1 \qquad \overline{\sigma}_{rrN} = 0 \\ &\overline{r} = \overline{r}_i \qquad \overline{\sigma}_{rri} = \overline{\sigma}_{rr,i+1} \qquad \overline{u}_{ri} = \overline{u}_{r,i+1} \qquad i = 1, 2, \ldots, N-1 \end{aligned} \tag{2.20}$$

The solution to Eq. (2.19) can be expressed by

$$\overline{u}_{ri} = \overline{u}_{ric} + \overline{u}_{rip} \tag{2.21}$$

where $\overline{u}_{ric}$ and $\overline{u}_{rip}$ denote the homogeneous and particular solution to Eq. (2.19), respectively. We now consider the homogeneous solution, and introduce the following equation

$$\overline{r} = \exp(s) \tag{2.22}$$

Changing a variable with the use of Eq. (2.22), the homogeneous equation of Eq. (2.19) reduces to

$$\Big[\frac{d^2}{ds^2} + l_i\frac{d}{ds} - (1 - \nu_i l_i)\Big]\overline{u}_{ric} = 0 \tag{2.23}$$

The homogeneous solution $\overline{u}_{ric}(\overline{r})$ for $i = 2, \ldots, N$ is given by

$$\overline{u}_{ric} = A_{1i}\exp(\Lambda_{i1}s) + A_{2i}\exp(\Lambda_{i2}s) = A_{1i}\overline{r}^{\Lambda_{i1}} + A_{2i}\overline{r}^{\Lambda_{i2}} \qquad i = 2, \ldots, N \tag{2.24}$$

where

$$\Lambda_{i1} = \frac{1}{2}\Big[-l_i + \sqrt{l_i^2 + 4(1-\nu_i l_i)}\Big] \qquad \Lambda_{i2} = \frac{1}{2}\Big[-l_i - \sqrt{l_i^2 + 4(1-\nu_i l_i)}\Big] \tag{2.25}$$

The particular solution $\overline{u}_{rip}$ for $i = 2, \ldots, N$ also can be obtained as follows

$$\begin{aligned}
\overline{u}_{rip} = {} & \frac{1}{\sqrt{l_i^2 + 4(1-\nu_i l_i)}}\Big\{ C_{a1}^{(i)}[-L_{a1a}^{(i)}(\overline{r})\overline{r}^{\Lambda_{i2}} + L_{a1b}^{(i)}(\overline{r})\overline{r}^{\Lambda_{i1}}] \\
& + C_{a2}^{(i)}[-L_{a2a}^{(i)}(\overline{r})\overline{r}^{\Lambda_{i2}} + L_{a2b}^{(i)}(\overline{r})\overline{r}^{\Lambda_{i1}}] \\
& + C_{b1}^{(i)}[-L_{b1a}^{(i)}(\overline{r})\overline{r}^{\Lambda_{i2}} + L_{b1b}^{(i)}(\overline{r})\overline{r}^{\Lambda_{i1}}] + C_{b2}^{(i)}[-L_{b2a}^{(i)}(\overline{r})\overline{r}^{\Lambda_{i2}} + L_{b2b}^{(i)}(\overline{r})\overline{r}^{\Lambda_{i1}}] \\
& + \sum_{j=1}^{\infty}\Big\{ C_{c1j}^{(i)}[-L_{c1ja}^{(i)}(\overline{r})\overline{r}^{\Lambda_{i2}} + L_{c1jb}^{(i)}(\overline{r})\overline{r}^{\Lambda_{i1}}] + C_{c2j}^{(i)}[-L_{c2ja}^{(i)}(\overline{r})\overline{r}^{\Lambda_{i2}} + L_{c2jb}^{(i)}(\overline{r})\overline{r}^{\Lambda_{i1}}] \\
& + C_{d1j}^{(i)}[-L_{d1ja}^{(i)}(\overline{r})\overline{r}^{\Lambda_{i2}} + L_{d1jb}^{(i)}(\overline{r})\overline{r}^{\Lambda_{i1}}] + C_{d2j}^{(i)}[-L_{d2ja}^{(i)}(\overline{r})\overline{r}^{\Lambda_{i2}} + L_{d2jb}^{(i)}(\overline{r})\overline{r}^{\Lambda_{i1}}]\Big\}\Big\}
\end{aligned} \tag{2.26}$$

The expressions for $C_{a1}^{(i)}$, $L_{a1a}^{(i)}(\overline{r})$ and so on in Eq. (2.26) are omitted here for the sake of brevity. On the other hand, the solution $\overline{u}_{ri}$ for $i = 1$ is

$$\overline{u}_{ri} = A_{1i}\overline{r} + \frac{(1+\nu_i)\overline{\alpha}_i}{\overline{r}} \int_0^{\overline{r}} \overline{r}\overline{T}_i \, d\overline{r} \tag{2.27}$$

The coefficients A_{1i} and A_{2i} in Eqs. (2.24) and (2.27) are unknown constants. Then, the stress components can be evaluated by substituting Eqs. (2.21), (2.24), (2.26) and (2.27) into Eq. (2.12), and later into Eq. (2.13). The unknown constants in Eqs. (2.24) and (2.27) can be determined so as to satisfy boundary conditions (2.20).

3. Numerical results

We consider the FGMs composed of titanium alloy (Ti-6Al-4V) and zirconium oxide (ZrO_2). The FGM disk is heated from the outer surface (zirconium oxide 100%) by surrounding media, and is cooled from both flat surfaces. The material of the first inner layer $(i = 1)$ is titanium alloy 100% and the material at the outer surface is zirconium oxide. The material properties g_i of the interface between the ith and $(i+1)$th layer are assumed as follows

$$g_i = g_a + (g_b - g_a)f_i \qquad 0 \leqslant f_i \leqslant 1 \qquad i = 2, \ldots, N-1 \tag{3.1}$$

where g_a is the material property of the first inner layer, and g_b is the material property of the outer surface. The heat capacity per unit volume $c_i\rho_i$ and Poisson's ratio ν_i of the ith layer use the average of values in both interfaces. The numerical parameters of heat conduction, shape and f_i are presented as follows

$$H_b = 10.0 \qquad H_{si} = 0.1 \qquad \overline{T}_b = 1.0 \qquad \overline{B} = 0.05 \tag{3.2}$$

Case 1: $N = 3$

$$\overline{r}_1 = 0.1 \qquad \overline{r}_2 = 0.55 \qquad f_2 = 0.1,\ 0.5,\ 0.9 \tag{3.3}$$

Case 2: $N = 4$

$$\begin{aligned}
&\overline{r}_1 = 0.1 \qquad \overline{r}_2 = 0.4 \qquad \overline{r}_3 = 0.7 \\
&f_2 = 0.1 \qquad f_3 = 0.2,\ 0.5,\ 0.9
\end{aligned} \tag{3.4}$$

The material constants for titanium alloy (Ti-6Al-4V) are taken as:
— for titanium alloy (Ti-6Al-4V)

$$\begin{aligned} &\kappa = 2.61 \cdot 10^{-6}\,\mathrm{m^2/s} && c = 537.7\,\mathrm{J/(kg \cdot K)} && \rho = 4420\,\mathrm{kg/m^3} \\ &\lambda = 6.2\,\mathrm{W/(m \cdot K)} && \alpha = 8.9 \cdot 10^{-6}\,\mathrm{1/K} && E = 105.8\,\mathrm{GPa} \qquad \nu = 0.3 \end{aligned} \tag{3.5}$$

— for zirconium oxide (ZrO_2)

$$\begin{aligned} &\kappa = 1.06 \cdot 10^{-6}\,\mathrm{m^2/s} && c = 461.4\,\mathrm{J/(kg \cdot K)} && \rho = 3657\,\mathrm{kg/m^3} \\ &\lambda = 1.78\,\mathrm{W/(m \cdot K)} && \alpha = 8.7 \cdot 10^{-6}\,\mathrm{1/K} && E = 116.4\,\mathrm{GPa} \qquad \nu = 0.3 \end{aligned} \tag{3.6}$$

The typical values of material properties such as κ_0, λ_0, α_0 and E_0 used to normalize the numerical data, are based on those of zirconium oxide.

In order to assess the influence of the material property distribution for three-layered FGM model, the numerical results for Case 1 are shown in Figs. 1 and 2. Figure 1a shows the variation of temperature change along the radial direction. Figure 1b shows the variation of the displacement $\overline{u}_r$ along the radial direction. From Figs. 1a and 1b, it is seen that the temperature and displacement rise as time proceeds and they are the greatest in the steady state. It can be seen from Figs. 1a and 1b that the values of the temperature change at the center of the solid disk and the displacement decrease when the parameter f_2 increases. Figures 2a and 2b show the variations of thermal stresses $\overline{\sigma}_{rr}$ and $\overline{\sigma}_{\theta\theta}$ along the radial direction, respectively. From Fig. 2, the maximum tensile stress occurs in the transient state near the center of the solid circular disk. It can be seen from Fig. 2 that the maximum values of the thermal stresses $\overline{\sigma}_{rr}$ and $\overline{\sigma}_{\theta\theta}$ decrease when the parameter f_2 decreases.

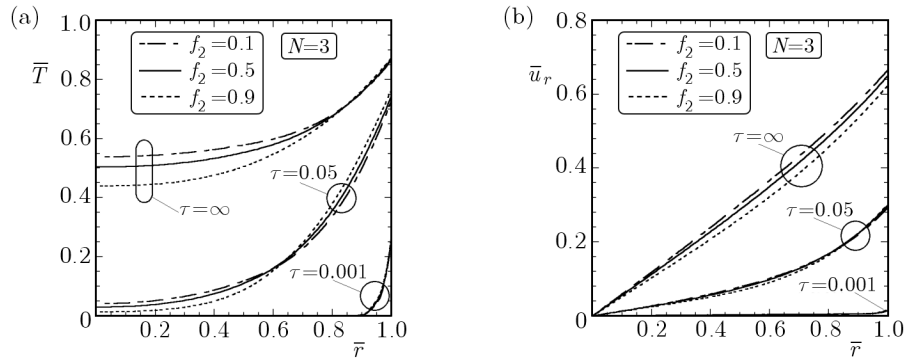

Fig. 1. Variation of temperature change (a) and of displacement $\overline{u}_r$ (b) in the radial direction (Case 1, $N = 3$)

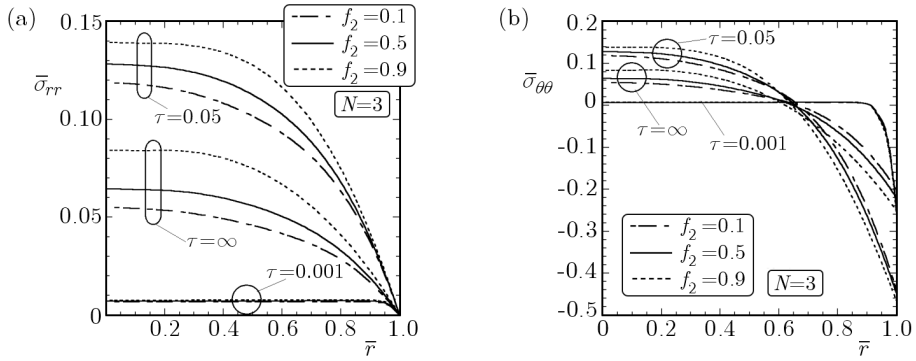

Fig. 2. Variation of thermal stresses in the radial direction (Case 1, $N = 3$): (a) radial stress $\overline{\sigma}_{rr}$ and (b) hoop stress $\overline{\sigma}_{\theta\theta}$

In order to assess the influence of the material property distribution for the four-layered FGM model, the numerical results for Case 2 are shown in Fig. 3. Figures 3a and 3b show the variations of thermal stresses $\overline{\sigma}_{rr}$ and $\overline{\sigma}_{\theta\theta}$, respectively. It can be seen from Fig. 3 that the maximum values of thermal stresses $\overline{\sigma}_{rr}$ and $\overline{\sigma}_{\theta\theta}$ decrease when the parameter f_3 decreases.

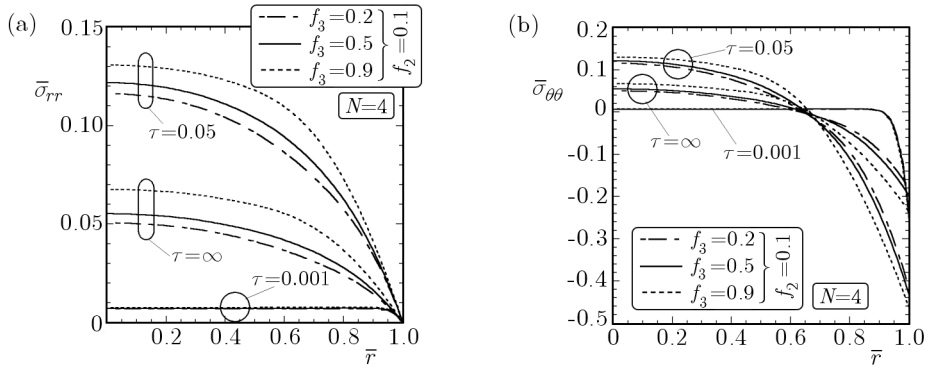

Fig. 3. Variation of thermal stresses in the radial direction (Case 2, $N = 4$): (a) radial stress $\overline{\sigma}_{rr}$ and (b) hoop stress $\overline{\sigma}_{\theta\theta}$

4. Conclusion

We analyzed the transient thermoelastic problem involving a functionally graded solid circular disk with piecewise power law due to uniform heat supply from the outer surface. The FGM circular disk is also cooled from the upper and lower surfaces of each layer with a constant heat transfer coefficient. The thermal conductivity, Young's modulus and the coefficient of linear thermal expansion of each layer, except the first inner layer, are expressed as power functions of the radial coordinate in the radial direction, and their values continue on each interface. We obtained the exact solution for the transient one-dimensional temperature and transient thermoelastic response of the FGM circular disk. We carried out numerical calculations for the FGMs composed of titanium alloy (Ti-6Al-4V) and zirconium oxide (ZrO_2) and examined the behavior in the transient state for the temperature change, displacement, and thermal stresses. Furthermore, the influence of the functional gradation on the temperature and thermoelastic response was investigated.

References

1. Guo L.C., Noda N., 2007, Modeling method for a crack problem of functionally graded materials with arbitrary properties – piecewise-exponential model, *Int. J. Solids Struct*, **44**, 6768-6790
2. Noda N., Tsuji T., 1991, Steady thermal stresses in a plate of functionally gradient material, *Trans. Jpn. Soc. Mech. Eng.*, **57A**, 98-103
3. Obata Y., Noda N., 1995, Transient thermal stresses in a hollow sphere of functionally gradient material, *Proc. First Int. Sympo. Thermal Stresses and Related Topics*, 335-338
4. Ohmichi M, Noda N, Ishihara M., 2010, The effect of oblique functional gradation to transient thermal stresses in the functionally graded infinite strip, *Acta Mech.*, **212**, 219-232
5. Ootao Y., 2010, Transient thermoelastic analysis for a multilayered hollow cylinder with piecewise power law nonhomogeneity, *J. Solid Mech. Mater. Eng.*, **4**, 1167-1177
6. Ootao Y., Akai T., Tanigawa Y., 1995, Three-dimensional transient thermal stress analysis of a nonhomogeneous hollow circular cylinder due to a moving heat source in the axial direction, *J. Thermal Stresses*, **18**, 497-512

7. Ootao Y., Tanigawa Y., 1994, Three-dimensional transient thermal stress analysis of a nonhomogeneous hollow sphere with respect to rotating heat source, *Trans. Jpn. Soc. Mech. Eng.*, **60A**, 2273-2279
8. Ootao Y., Tanigawa Y., 1999, Three-dimensional transient thermal stresses of functionally graded rectangular plate due to partial heating, *J. Thermal Stresses*, **22**, 35-55
9. Ootao Y., Tanigawa Y., 2005, Three-dimensional solution for transient thermal stresses of functionally graded rectangular plate due to nonuniform heat supply, *Int. J. Mech. Sci.*, **47**, 1769-1788
10. Ootao Y., Tanigawa Y., 2006, Transient thermoelastic analysis for a functionally graded hollow cylinder, *J. Thermal Stresses*, **29**, 1031-1046
11. Peng X.L., Li X.F., 2010, Thermal stress in rotating functionally graded hollow circular disks, *Comp. Struct.*, **92**, 1896-1904
12. Shao Z.S., Wang T.J., Ang K.K., 2007, Transient thermo-mechanical analysis of functionally graded hollow circular cylinders, *J. Thermal Stresses*, **30**, 81-104
13. Sugano Y., 1987, An expression for transient thermal stress in a nonhomogeneous plate with temperature variation through thickness, *Ing. Arch.*, **57**, 147-156
14. Sugano Y., Chiba R., Hirose K., 2001, Analytical solutions of transient temperature and thermal stress in a circular plate with arbitrary variation of heat-transfer coefficient, *Trans. Jpn. Soc. Mech. Eng.*, **67A**, 542-548
15. Tanigawa Y., Fukuda T., Ootao Y., Tanimura S., 1989, Transient thermal stress analysis of a multilayered composite laminate cylinder with a uniformly distributed heat supply and [its analytical development to nonhomogeneous materials], *Trans. Jpn. Soc. Mech. Eng.*, **55A**, 1133-1139
16. Vel S.S., Batra C., 2003, Three-dimensional analysis of transient thermal stresses in functionally graded plates, *Int. J. Solids Struct.*, **40**, 7181-7196
17. Zhao J., Ai X., Li Y., Zhou Y., 2006, Thermal shock resistance of functionally gradient solid cylinders, *Mater. Sci. Eng. A*, **418**, 99-110

Analiza stanu nieustalonego termosprężystości kołowego dysku wykonanego z materiału gradientowego opisanego modelem kawałkami potęgowym

Streszczenie

W pracy przedstawiono analizę procesów nieustalonych termosprężystości zachodzących w kołowym dysku wykonanym z materiału gradientowego opisanego modelem matematycznym opartym na funkcji kawałkami potęgowej przy założeniu jednorodnego ogrzewania od strony zewnętrznej. Badany dysk jest jednocześnie chłodzony na górnej i dolnej płaskiej powierzchni. Struktura dysku zawiera wiele kołowych warstw gwarantujących dowolność kształtowania właściwości materiału w zależności od położenia. Współczynnik przewodnictwa cieplnego, moduł Younga oraz współczynnik liniowej rozszerzalności cieplnej każdej warstwy, oprócz pierwszej, wyrażono w postaci funkcji potęgowych współrzędnej promieniowej przy zachowaniu warunków zgodności między warstwami. Otrzymano dokładne rozwiązanie dla stanu nieustalonego termosprężystości wywołanego jednowymiarową zmianą temperatury oraz określono zachowanie się materiału poddanego płaskiemu stanowi naprężenia. Wybrane rezultaty badań dotyczące zmian temperatury oraz rozkładów naprężeń i przemieszczeń przedstawiono graficznie.

Manuscript received January 25, 2012; accepted for print February 6, 2012